Higher Harmonic Oscillations in a Noncontacting FMR Mechanical Face Seal Test Rig

An Sung Lee

Itzhak Green[1]

Woodruff School of Mechanical Engineering,
Georgia Institute of Technology,
Atlanta, GA 30332

In order to investigate experimentally the dynamic behavior of a noncontacting flexibly mounted rotor (FMR) mechanical face seal a test rig was designed and built. Test results showed that the FMR seal was vulnerable to higher harmonic oscillations with frequencies that are integer multiples of the shaft speed. Because system nonlinearities can cause higher harmonic oscillations, the dynamic moments acting on the rotor are derived to include the effects of imbalance and axial offset of the rotor. The analysis reveals that the nonlinear terms involved are of second order and generally can be neglected. Investigation is then directed to analyze the possibility of rubbing contact between the rotor and the stator. Rubbing contact can occur as a result of a high relative angular misalignment between the rotor and the stator. A contact kinematics model is proposed and a Fourier series analysis is performed on the resulting rotor response. The analysis shows that the proposed response contains higher harmonics. Fourier series expansion and numerical filtering of a sampled rotor response from the test rig yield resembling signals which contain higher harmonics. This suggests that rubbing contact is the source of higher harmonic oscillations. Design modification to the rotor flexible support system resulted in a virtual elimination of higher harmonic oscillations.

Introduction

Mechanical face seals are commonly used in applications that demand tightly controlled leakage rates. High speeds, pressures, and temperatures in high performance rotating machinery mandate the utilization of noncontacting seals for long lasting and reliable operation. In a noncontacting seal a thin fluid film lubricates the seal faces, consequently reducing friction loses and wear. A good understanding of the seal dynamics is essential for designing reliable noncontacting operation with minimum leakage.

Seal dynamics has been an active area of research (Etsion, 1982, 1985, and 1991; and Allaire, 1984). Etsion and Burton (1979) tested a face seal model consisting of a rigidly mounted rotor and a flexibly mounted stator (FMS) under eccentric loading, i.e., initial stator misalignment. Self-excited oscillations in the form of combined precession and nutation of the stator were observed. Etsion and Constantinescu (1984) experimentally observed the dynamic behavior of a noncontacting FMS mechanical face seal. They showed that the stator misalignment and its phase shift are time dependent. Green and Etsion (1985, 1986) analyzed the dynamic behavior of a noncontacting FMS mechanical face seal and the analysis was shown to be valid in many practical cases.

Theoretical work on the dynamics of a noncontacting flexibly mounted rotor (FMR) mechanical face seal was performed by Green (1989, 1990). That work showed that the FMR seal is inherently stable regardless of operating speed, provided that the inertia ratio, I_t/I_p (transverse moment of inertia over polar moment of inertia), is less than one, which is a practical ratio in most mechanical face seals. Further, the FMR seal was found to be a better design than the FMS seal in terms of various seal performance criteria, i.e., the total relative misalignment, critical stator misalignment, and threshold speed of instability in the case where the inertia ratio is greater than one. Analytical steady-state solution was given in terms of transmissibilities (amplitude ratio of response over forcing input). However, no experimental investigation of a noncontacting FMR mechanical seal has been reported. In order to investigate experimentally the dynamic behavior of the FMR seal a test rig was designed and built.

In the test rig the rotor was expected to have a sinusoidal response with a frequency equal to the shaft rotating frequency. This is because the rotor is responding to a sinusoidal forcing function in the form of the initial rotor misalignment (Green, 1989). However, the experimental results as obtained from the test rig showed that the FMR seal was vulnerable to higher harmonic oscillations, where superimposed signals of integer multiples of the shaft rotating frequency were observed. Such oscillations in triboelements in general, and mechanical face seals in particular, may indicate imminent failure. The purpose of this work is to identify and investigate the source of higher harmonic oscillations and to offer a remedy to the problem.

[1]Currently with Technion Israel Institute of Technology, Haifa, Israel

Contributed by the Technical Committee on Vibration and Sound for publication in the JOURNAL OF VIBRATION AND ACOUSTICS. Manuscript received April 1993. Associate Technical Editor: I. Grahim.

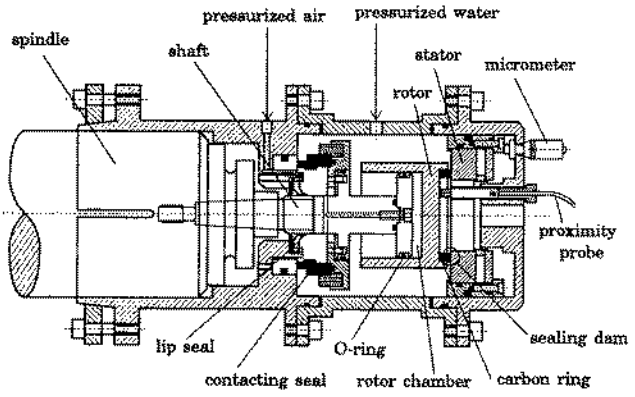

Fig. 1 Noncontacting FMR mechanical face seal test rig

One source of higher harmonic oscillations is nonlinear excitation. When a nonlinear system is excited by a sinusoidal input, its steady state output is often periodic with a distorted shape due to sub or higher harmonic oscillations (Crandall, 1974). To investigate the possibility of a nonlinear response the dynamic moments acting on the rotor are derived to include the effects that produce nonlinear terms, namely, imbalance and axial offset.

The problem of higher harmonic oscillations in rotating machinery has been tackled by other researchers. Misalignment effects of bent shafts and improperly seated bearings, and mechanical looseness of mounts and bearings, were documented by Rao (1983) and Vance (1988). Asymmetric shaft problems were documented by Rao (1983) and Vance (1988), and investigated by Muszynska (1989). Rotor and stator rubbing problems of seals were investigated by Beatty (1985), and documented by Vance (1988).

In the present test rig contact is suspected to occur in the axial direction due to a high relative angular misalignment between the rotor and the stator. A Fourier series expansion contains frequencies which are integer multiples of the fundamental frequency. Therefore, a Fourier analysis will be used to analyze the presence of higher harmonic oscillations. Finally, an improved rotor response following design modifications will be discussed.

Test Rig and Results

A schematic of the test rig is shown in Fig. 1. A sealing dam is formed between the faces of the stator and the carbon ring that is attached to the rotor. The rotor inertia properties are $m = 0.52$ kg, $I_t = 2.80 \times 10^{-4}$ kg·m^2, and $I_p = 4.16 \times 10^{-4}$ kg·m^2. The carbon ring has an O.D. of 50.8 mm and an I.D. of 40.64 mm. Separation of the two faces was achieved by utilizing the hydrostatic effect that prevails in a converging gap between the flat-face carbon ring and the coned-face stator. The rotor was flexibly mounted on the shaft by means of an elastomeric Nitrile (Buna N) O-ring to allow its tracking to the stator misalignment. The geometric balance ratio was calculated to be 0.5, assuming a flat-face seal and that the closing force (at the back side of the rotor) and the opening force (at the sealing dam) are equal. This ratio allowed for easy control of the seal clearance by varying the closing force by supplying air pressure to the rotor chamber through holes in the shaft and housing. Thus, various seal clearances at the sealing dam could be obtained by varying the air pressure. The pressurized air and the pressurized water were separated by a contacting mechanical seal at one end, whereas the pressurized air was sealed by a lip seal at the other end. The shaft was screwed into a precision spindle which was driven by a motor mounted on a separate structure through a wafer spring coupling. The stator misalignment was adjusted by three micrometers, and the dynamic behavior of the rotor was detected by three eddy current proximity probes whose signals were sampled by a data acquisition system. The data acquisition system consisted of a personal computer equipped with a real-time data acquisition board and software. Leakage was measured by a flow meter placed on the supply line of the pressurized water.

Tests were performed at a shaft speed of 30 Hz, coning angle of 7.2 mrad, water pressure of 0.21 MPa, and a mean seal clearance of 3.8 μm (coning is a measure of face taper in the radial direction, Green, 1987). The seal clearance was determined from the leakage equation (Etsion and Constantinescu, 1984),

$$Q = \frac{\pi p}{6\mu} C^3 \overline{Q} \tag{1}$$

where Q is the leakage, p is the pressure differential across the seal face, C is the seal clearance at the centerline, and $\overline{Q}$ is the dimensionless leakage. For a narrow seal $\overline{Q}$ can be expressed in the form (Etsion and Sharoni, 1980)

$$\overline{Q} = \frac{R_m}{1-R_i}\left[1 + \frac{3}{2}\bar{\gamma}^2 R_i + \frac{3}{2}\bar{\beta}(1-R_i)\left(1 + \frac{2}{3}\bar{\gamma}^2\frac{R_i^2}{R_m}\right)\right] \tag{2}$$

R_i is the seal inner to outer radius ratio, $R_i = r_i/r_o$, and $R_m = (1+R_i)/2$. $\bar{\gamma}$ is the dimensionless relative misalignment, $\bar{\gamma} = \gamma r_o/C$, where γ is the relative misalignment between the rotor and the stator. $\bar{\beta}$ is the dimensionless coning, $\bar{\beta} = \beta r_o/C$, where β is the coning angle on the stator face. Following the recommendation by Etsion and Constantinescu (1984) it was assumed that γ is negligible. In such case $\overline{Q}$ reduces to

$$\overline{Q} = \frac{R_m}{1-R_i}\left[1 + \frac{3}{2}\bar{\beta}(1-R_i)\right] \tag{3}$$

Because of the various assumptions $\overline{Q}$ in Eq. (3) contains some error. But the error in calculating C [using Eqs. (1) and (3)] will be much smaller because a cubic root is taken on $\overline{Q}$.

A sample of the rotor response as measured by one probe and its power spectrum are shown in Figs. 2 and 3, respectively. In Fig. 2 the zero value line represents the mean value of the rotor response, i.e., analogous to the elimination of a DC level offset. Higher harmonics in the form of integer multiples of

Nomenclature

C = seal clearance, or rotor centroid
d = axial offset, the distance between C and O along z
G = rotor center of mass
I_t, I_p = transverse and polar moments of inertia
m = rotor mass
O = origin of the coordinate systems, $\xi\eta\zeta$, XYZ, and xyz
t = time
XYZ = rotating reference system
xyz = rotor reference system
α = relative precession of ϵ with respect to x
α_r = absolute precession of ϵ with respect to ξ, $\psi_r + \alpha$
γ_r = rotor angular response, the nutation about x
γ_ξ, γ_η = components of γ_r in the $\xi\eta\zeta$ system
ϵ = imbalance, the distance between G and C parallel to the xy plane
$\xi\eta\zeta$ = inertial reference system
θ = half of contact arc
ψ = relative precession of x with respect to X
ψ_r = absolute precession of x with respect to ξ, $\omega t + \psi$
ω = shaft speed

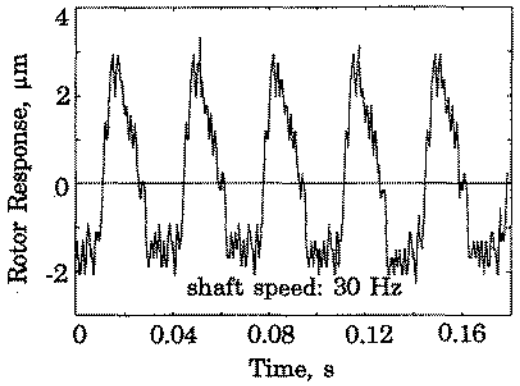

Fig. 2 Axial rotor response measured by one probe

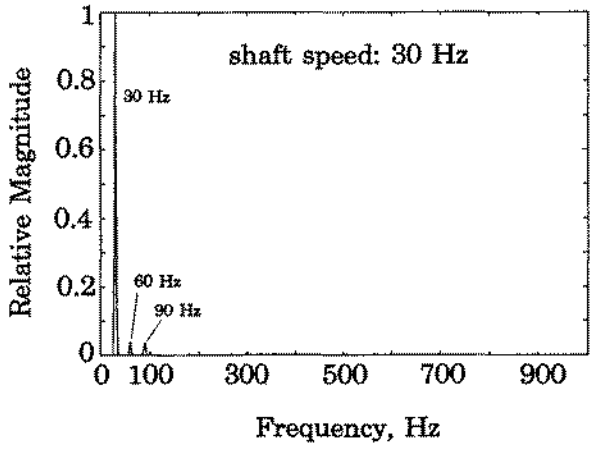

Fig. 3 Power spectrum of the rotor response

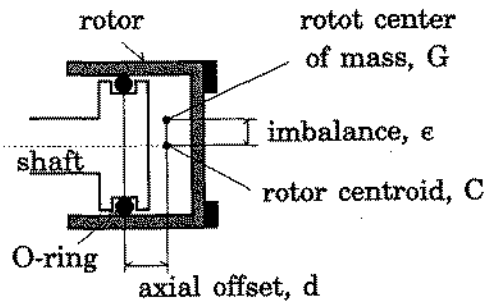

Fig. 4(a) Imbalance and axial offset of rotor

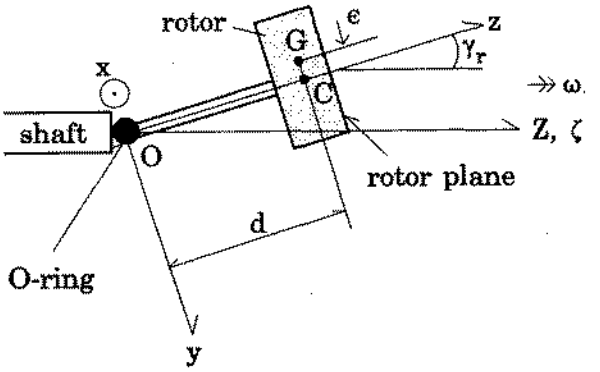

Fig. 4(b) Dynamic model of rotor

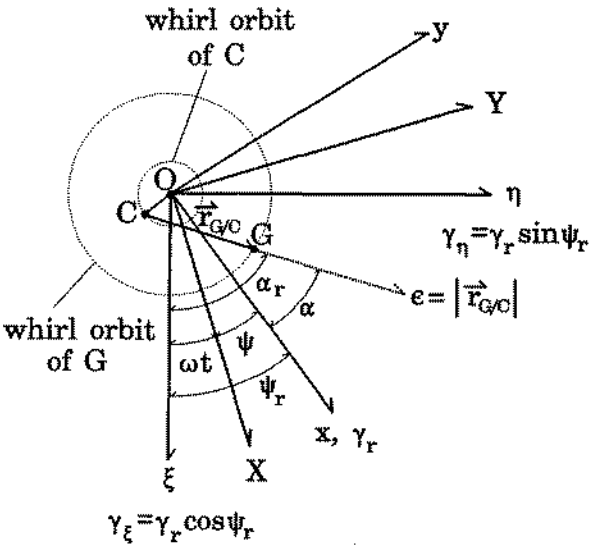

Fig. 5 Coordinates systems and vectors

the shaft speed, 30 Hz, are observed in Fig. 3. Tests at other shaft speeds, e.g., 10, 15, 20, and 25 Hz, produced power spectra similar to that in Fig. 3. While in all test runs the power spectrum magnitude of the fundamental frequency was always the largest, the higher harmonics varied in their power spectrum magnitudes and occurrences. At times their magnitudes reached up to 40 percent of the fundamental frequency, where at other times a certain higher harmonic had no visible magnitude at all. To exclude the possibility of instability as being the source of nonsynchronous oscillations, it is noted that the whirling speed of the FMR seal at the transition mode from stable to unstable operation was found to be approximately half of the shaft speed (Green, 1990). The absence of a half-frequency component in the power spectrum indicates that instability is not the cause of the problem. The periodic nature of the response indicates that the observed higher harmonic oscillations originate from the system operation at steady-state rather than from a random noise source.

Any of the test rig components in relative motion, in particular the spindle bearings and the contacting seal, could be the source of the higher harmonic oscillations. Series of tests were performed in which suspected components were isolated one at a time. When the water was drained out, tests were performed with only the stator removed, and then also with the contacting seal removed. All these tests produced virtually pure single-frequency sinusoidal rotor responses, as required. Therefore, neither the spindle bearings nor the contacting seal were considered to be the sources of the higher harmonic oscillations. This leaves either a nonlinear rotor behavior, or rubbing contact at the rotor-stator interface (once the stator is replaced) as the sources of said oscillations. The subsequent analysis is aimed at these two sources.

Analysis

Nonlinearity in the Dynamic Moments. Green (1990) derived the dynamic moments acting on the noncontacting FMR seal based on the assumptions that there is no imbalance, and that the rotor center of mass coincides with the centroid. To investigate the possibility of nonlinear behavior of the rotor, however, the dynamic moments acting on the rotor need to be rederived to include the effects that produce nonlinear terms, namely, the imbalance, ϵ, and the axial offset, d (Fig. 4). In the test rig the rotor angular response (rotor nutation), γ_r, is very small (order of 10^{-4} rad) such that the various tilts can be treated as plane vectors (Fig. 5). A detailed derivation of the dynamic moments, ultimately expressed in the inertial $\xi\eta\zeta$

system, is given in the Appendix. The final result, Eq. (A8), is

$$\Sigma \mathbf{M}_C = \begin{Bmatrix} (I_t + md\epsilon\gamma_r \sin\alpha)\ddot{\gamma}_\xi + I_p\omega\dot{\gamma}_\eta \\ (I_t + md\epsilon\gamma_r \sin\alpha)\ddot{\gamma}_\eta - I_p\omega\dot{\gamma}_\xi \\ -md\epsilon(\ddot{\gamma}_\xi \cos\alpha_r + \ddot{\gamma}_\eta \sin\alpha_r) \end{Bmatrix}_{\xi\eta\zeta} \tag{4}$$

where, respectively, I_t and I_p are the transverse and polar moments of inertia of the rotor at point C in the xyz system, γ_ξ and γ_η are the two components of γ_r in the inertial $\xi\eta\zeta$ system, α and α_r are the relative and absolute precessions of ϵ with respect to x and ξ, and ω is the shaft speed. The nonlinearity is due to $\gamma_r\ddot{\gamma}_\xi$ and $\gamma_r\ddot{\gamma}_\eta$, which are second order terms. As such they can generally be neglected. (Note, however, that the nonlinear terms are multiplied by d and ϵ. A good design should not tolerate large d or ϵ. In the present test rig $md\epsilon\gamma_r/I_t$ is of order 10^{-5} assuming generous axial offset and imbalance, $d = 5$ mm and $\epsilon = 1$ mm, respectively.) Since the nonlinear terms drop out, the dynamic moments about ξ and η of Eq. (4) reduce to

$$\begin{aligned} (\Sigma M_C)_\xi &= I_t\ddot{\gamma}_\xi + I_p\omega\dot{\gamma}_\eta \\ (\Sigma M_C)_\eta &= I_t\ddot{\gamma}_\eta - I_p\omega\dot{\gamma}_\xi \end{aligned} \tag{5}$$

The linear Eqs. (5) are the same as those derived by Green (1990). Hence, a linearized dynamic analysis of the FMR seal is justified even when some ϵ and d are present. It is concluded that the nonlinearity in the dynamic moments is negligible and, therefore, it is not likely to be the source of higher harmonic oscillations. However, the dynamic torque, $(\Sigma M_C)_\zeta$, of Eq. (4) is of first order, and may cause slip between the rotor and the shaft if the circumferential friction of the O-ring is not sufficient. Since the troubleshooting procedure and the nonlinear analysis rendered a negative prognosis as to the source of higher harmonic oscillations, it leaves rubbing contact between the rotor and the stator as the sole potential source of the problem.

Rubbing Contact Between Rotor and Stator. Although the seal was designed to operate in a noncontacting regime, potential contact between the rotor and the stator needs to be considered. As discussed previously contact is possible due to a high relative misalignment between the rotor and the stator. The relative misalignment between the rotor and the stator, γ, is a rotating vector of varying relative frequency, $\dot{\varphi}$ (Green, 1989). The magnitudes of both γ and $\dot{\varphi}$ vary cyclically at ω. Similarly, the seal clearance, C, varies cyclically at ω. The leakage as measured by the flow meter is an averaged value, and thereby, C [which is determined from the leakage, Eqs. (1) and (3), while assuming that $|\gamma|$ is negligible], is also an averaged value. However, when contact occurs between the rotor and the stator, $|\gamma|$ is no longer negligible and C determined from the leakage cannot be considered credible. For this reason the seal clearance as calculated from the leakage cannot be used to prove whether contact occurs or not, especially when contact is suspected.

Often the rotor responses as measured by one or two probes were like the one in Fig. 2, where the remaining probes exhibited sinusoidal signals. This indicates that contact may have occurred over some arc section of the stator face, with an arc extent that depends on $|\gamma|$. If one or two particular probes are surrounded by the contact arc section, then the rotor responses as measured by those probes will be like that in Fig. 2. These responses are analyzed by a contact kinematics model and a Fourier series analysis as follows.

A contact kinematics model of the rotor and the stator is proposed in Fig. 6(*a*). In the side view, Fig. 6(*b*), the contact arc, 2θ, represents a contact portion of the stator face. If we suppose that a probe is located along the center line of the

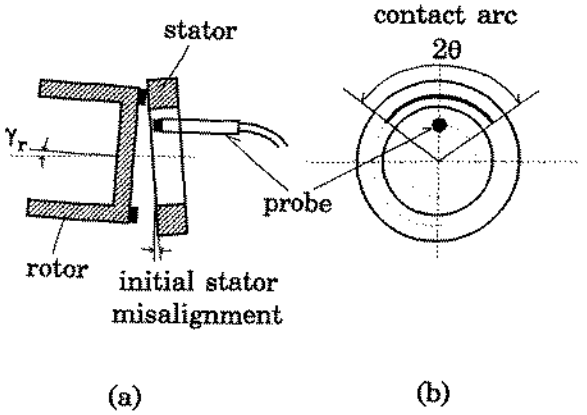

Fig. 6(*a*) Contact kinematics of rotor and stator
Fig. 6(*b*) Contact arc and probe position

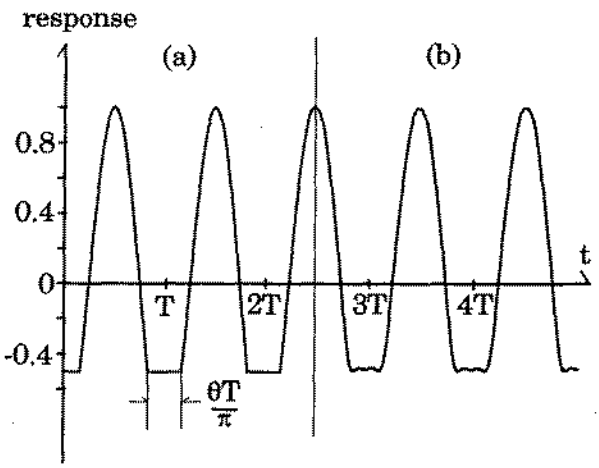

Fig. 7(*a*) Proposed rotor response under contact
Fig. 7(*b*) Fourier series expansion with n summed up to 6

contact arc, then a rotor response measured by that probe would be like the one in Fig. 7(*a*). A time interval of the truncated portion is $\theta T/\pi$, where T is a period of the shaft rotation. The proposed rotor response under contact conditions is expressed as a function of time as follows:

$$f(t) = -\cos\theta \text{ when } mT < t < mT + \frac{\theta T}{2\pi},$$

$$\text{or } (m+1)T - \frac{\theta T}{2\pi} < t < (m+1)T$$

$$f(t) = -\cos\left(\frac{2\pi}{T}t\right) \text{ when } mT + \frac{\theta T}{2\pi} < t < (m+1)T - \frac{\theta T}{2\pi}$$

$$\text{for } m = 0, 1, 2, 3, \ldots \tag{6}$$

where $m = 0$ represents the first cycle, $m = 1$ represents the second cycle, and so forth. The function $f(t)$ can be expanded by a Fourier series as

$$f(t) = a_0 + \sum_{n=1}^{\infty} a_n \cos\left(\frac{2\pi n}{T}t\right) \tag{7}$$

where a_0 and a_n are obtained by

$$\begin{aligned} a_0 &= \frac{2}{T}\int_0^{T/2} f(t)dt \\ a_n &= \frac{4}{T}\int_0^{T/2} f(t)\cos\left(\frac{2\pi n}{T}t\right)dt \end{aligned} \tag{8}$$

Substituting Eq. (6) into Eq. (8) results analytically in

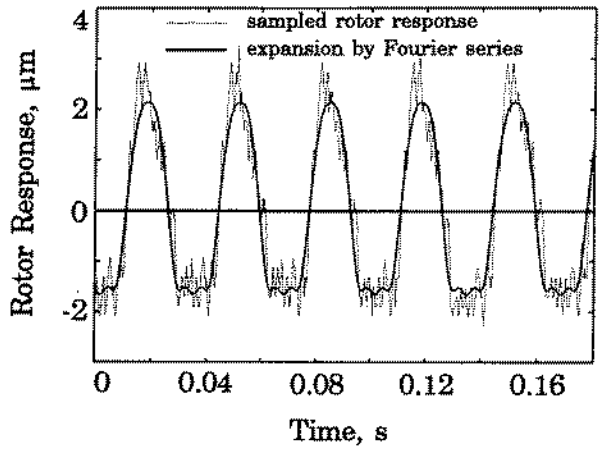

Fig. 8 Sampled rotor response from test rig and its expansion by Fourier series with n summed up to 6

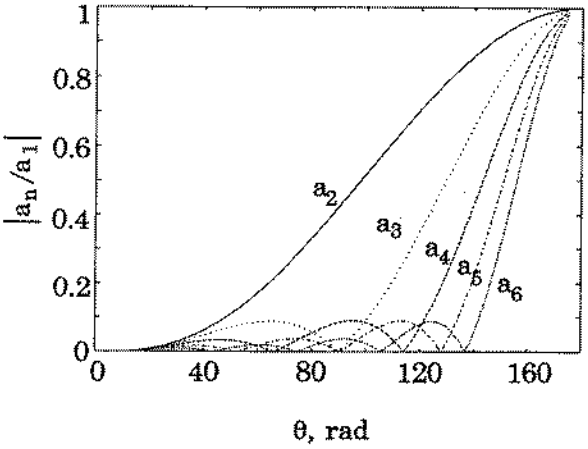

Fig. 10 Relative amplitudes of higher harmonics versus half of contact arc

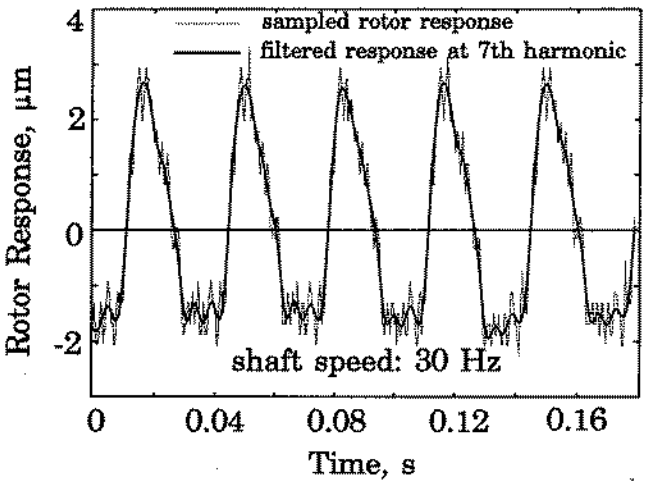

Fig. 9 Sampled rotor response from test rig and its filtered response at the seventh harmonic

$$a_0 = \frac{1}{\pi}(\sin\theta - \theta\cos\theta)$$

$$a_1 = -1 + \frac{\theta}{\pi} - \frac{1}{2\pi}\sin 2\theta$$

$$a_n = \frac{1}{\pi}\left[\frac{\sin(n-1)\theta}{n-1} - \frac{2\cos\theta\sin(n\theta)}{n} + \frac{\sin(n+1)\theta}{n+1}\right], \quad n = 2,3,4,\ldots \tag{9}$$

The above postulated analysis contains integer multiples of the shaft speed, $2\pi n/T$ ($=n\omega$). Figure 7(b) shows an expansion of the proposed rotor response by Fourier series with n summed up to 6 in Eq. (7), for $\theta = 60$ deg.

The sampled rotor response from the test rig (Fig. 2) was expanded by Fourier series using numerical integration in Eq. (8). The magnitudes of the coefficients a_i represent the weight of each harmonic. For example, $|a_0|$ represents the mean value, $|a_1|$ represents the weight of the first harmonic, and so forth. The numerical values of a_i, $i=0$ to 6, are 0.0269, −2.0578, 0.3848, 0.2338, −0.0686, −0.0750, and −0.0455. The magnitudes of a_i relative to each other conform to the relative magnitudes of the power spectrum in Fig. 3. The expansion of the rotor response is shown in Fig. 8.

The same raw rotor response of Fig. 2 was filtered in the time domain at the seventh harmonic using the Butterworth numerical filter. The filtered response is shown in Fig. 9. It is apparent that the expanded responses, Figs. 7(b) and 8, and the filtered response, Fig. 9, are alike in shape. Evidence of contact was found upon disassembling of the test rig, where scratches were spread over a section of the stator face similarly to the one shown in Fig. 6(b).

Absolute relative amplitudes of higher harmonics, $|a_n/a_1|$ ($n=2$ to 6), from Eq. (9) versus θ are plotted in Fig. 10. The magnitudes $|a_n|$ vary depending on θ while $|a_1|$ is always the largest. It can be seen that $|a_n|$ are zero at a certain value of θ, and approach $|a_1|$ as θ goes to 180 deg (an impractical value for rigid faces). This dependence of a_n on θ may explain why the higher harmonics varied in their power spectrum magnitudes and occurrences as observed from one experiment to another.

Modifications and Results

Analysis of the test rig indicated that rubbing contact between the rotor and the stator was the source of higher harmonic oscillations. If rubbing contact prevails over an extended period of time the seal will eventually wear out and fail. Corrective measures to eliminate rubbing contact had to be taken because the FMR seal was intended for noncontacting operation.

It was suspected that one O-ring support was not sufficient to ensure a small rotor angular response. Also, the absence of a spring in the original design appeared to impede the rotor ability to restore its designed position after a likely occurrence of an angular disturbance. Therefore, a shaft head having the support system of two O-rings and one spring was built, Fig. 11(a). The O-rings, having an I.D. of 37.69 mm and a cross section diameter of 3.53 mm, were installed with five percent stretch and seven percent squeeze. In addition, a stator which allows for various coning angles was built, Fig. 11(b). Various coning angles could be obtained by adjusting the tightening torque on the bolts in the stator holder. High coning is desirable in this case because the hydrostatic effect increases the opening force between the rotor and the stator. The new coning angle was increased to 11.2 mrad. A rotor response obtained after all three design modifications, and its power spectrum, are shown in Fig. 12. The rotor response is remarkably improved where the higher harmonic components have practically been eliminated, indicating noncontacting operation.

The other two probes measured signals very similar to the one shown in Fig. 12. Two probes were placed on a diameter where the third probe was placed on a perpendicular diameter. The average value of the two probes having 180 deg phase between them provides the variation of the seal clearance, C,

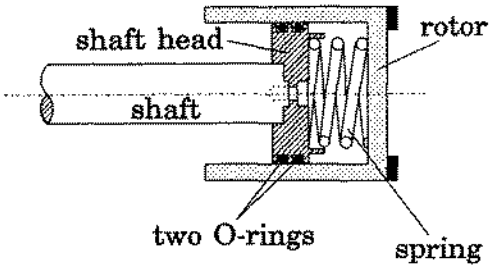

Fig. 11(*a*) Modified rotor support design

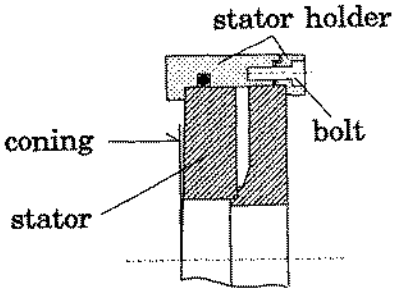

Fig. 11(*b*) Modified stator design

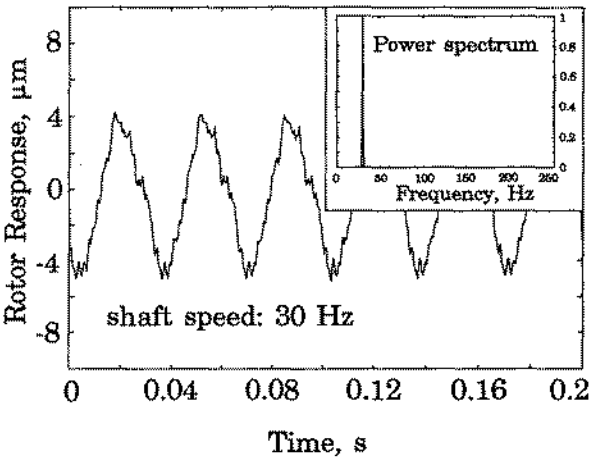

Fig. 12 Improved rotor response following design modifications and its power spectrum

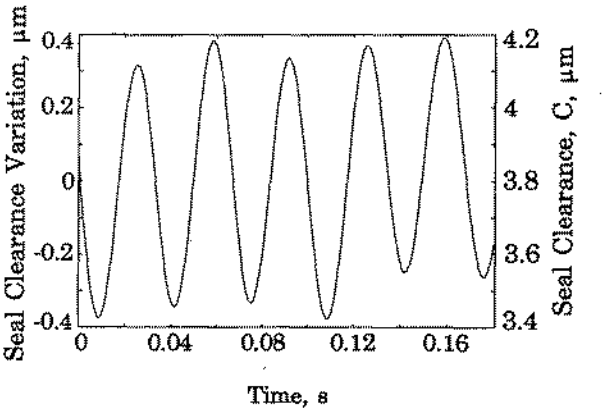

Fig. 13 Seal clearance variation as a function of time

at the seal centerline at a given instant. Figure 13 shows the variation with time (filtered signal) of C about the mean value of 3.8 μm [calculated from the leakage, Eq. (1)]. The shaft speed was 30 Hz, the coning angle was 11.2 mrad, and the water pressure was 0.21 MPa. It can be seen that the amplitude of oscillation is about 0.4 μm and that the frequency equals the shaft frequency. This oscillation is caused by the fixed stator and initial rotor misalignments. It is important to emphasize that this behavior is the result of the coupling between axial and angular degrees of freedom, since no forcing function exists in the axial mode. Therefore, the analysis by Green (1989) is incapable of predicting this behavior because the linearized rotordynamic coefficients, used in that analysis, have no such coupling. Only an investigation in which the complete nonlinear equations of motion are solved numerically can predict this behavior. Such an investigation was performed by Green and Etsion (1986b), but for an FMS seal (a nonlinear investigation for an FMR seal is not yet available). Indeed, Fig. 13 qualitatively agrees with Fig. 9 in the aforementioned reference. While the axial oscillation amplitude is only about 10 percent of the seal clearance [making the linearized approach by Green (1989) reasonable] its effect on the leakage is ± 27 percent [see Eq. (1)]. For this reason, obtaining the seal clearance from the leakage equation as an averaged value, as discussed following Eq. (3), is well justified.

Conclusions

Experimental results as obtained from the test rig showed that the FMR seal was vulnerable to higher harmonic oscillations in the form of integer multiples of the shaft speed. A derivation of the dynamic moments acting on the rotor revealed that a linearized dynamic analysis of the FMR seal is valid, even when some imbalance and axial offset of the rotor are present. After a process of elimination of the various test rig components it was determined that rubbing contact between the rotor and the stator was the source of higher harmonic oscillations.

A contact kinematics model between the rotor and the stator in the form of a truncated rotor response was proposed. A Fourier series analysis of the rotor response resulted in a continuous generation of higher harmonics. Furthermore, a Fourier series expansion and numerical filtering of a sampled rotor response were alike in shape and magnitude. It is concluded that the proposed rotor response under rubbing contact conditions provides a reasonable model for signals contaminated by higher harmonic oscillations. In order to eliminate rubbing contact design modifications were made, and thereafter, higher harmonic oscillations were negligible.

In order to understand an exciting mechanism of higher harmonic oscillations in the FMR seal and perform a complete stability analysis under contact conditions a kinetic study is required. This study should include the effects of rub-induced parametric forces and inertia.

Acknowledgment

This work was supported in part by the National Science Foundation under Grant Number MSM-8619190. This support is gratefully acknowledged. The authors would like to thank Mr. Ariel Trau and Dr. Scott Bair who helped in the design and construction of a prototype test rig. Mr. Trau spent his sabbatical leave from the Israel Armament Development Authority at the Georgia Institute of Technology.

References

Allaire, P. E., 1984, "Noncontacting Face seals for Nuclear Applications—A Literature Review," *Lubrication Engineering*, Vol. 40, No. 6, pp. 344–351.

Beatty, R. F., 1985, "Differentiating Rotor Response Due to Radial Rubbing," ASME Journal of Vibrations, Acoustics, Stress and Reliability in Design, Vol. 107, pp. 151–160.

Crandall, S. H., 1974, "Nonlinearities in Structural Dynamics," *The Shock and Vibration Digest*, Vol. 6, No. 8, pp. 2–14.

Etsion, I., and Burton, R. A., 1979, "Observation of Self-Excited Wobble in Face Seals," ASME *Journal of Lubrication Technology*, Vol. 101, No. 4, pp. 526–528.

Etsion, I., and Sharoni, A., 1980, "Performance of End-Face Seals with Diametral Tilt and Coning—Hydrostatic Effects," ASLE *Trans.*, Vol. 23, No. 3, pp. 279–288.

Etsion, I., 1982, "A Review of Mechanical Face Seal Dynamics," *The Shock and Vibration Digest*, Vol. 14, No. 4, pp. 9–14.

Etsion, I., and Constantinescu, I., 1984, "Experimental Observation of the Dynamic Behavior of Noncontacting Coned-Face Mechanical Seals," ASLE *Trans.*, Vol. 27, No. 3, pp. 263–270.

Etsion, I., 1985, "Mechanical Face Seal Dynamics Update," *The Shock and Vibration Digest*, Vol. 17, No. 4, pp. 11–15.

Etsion, I., 1991, "Mechanical Face Seal Dynamics 1985–1989," *The Shock and Vibration Digest*, Vol. 23, No. 4, pp. 3–7.

Green, I., and Etsion, I., 1985, "Stability Threshold and Steady-State Response of Noncontacting Coned-Face Seals," ASLE *Trans.*, Vol. 28, No. 4, pp. 449–460.

Green, I., and Etsion, I., 1986, "Nonlinear Dynamic Analysis of Noncontacting Coned-Face Mechanical Seals," ASLE *Trans.*, Vol. 29, No. 3, pp. 383–393.

Green, I., 1987, "The Rotor Dynamic Coefficients of Coned-Face Mechanical Seals with Inward or Outward Flow," ASME *Journal of Tribology*, Vol. 109, pp. 129–135.

Green, I., 1989, "Gyroscopic and Support Effects on the Steady-State Response of a Noncontacting Flexibly Mounted Rotor Mechanical Face Seal," ASME *Journal of Tribology*, Vol. 111, pp. 200–208.

Green, I., 1990, "Gyroscopic and Damping Effects on the Stability of a Noncontacting Flexibly-Mounted Rotor Mechanical Face Seal," *Dynamics of Rotating Machinery*, Hemisphere Publishing Company, pp. 153–173.

Muszynska, A., 1989, "Misalignment and Shaft Crack-Related Phase Relationships for 1X and 2X Vibration Components of Rotor Responses," *Orbit*, Vol. 10, No. 2, pp. 4–8.

Rao, J. S., 1983, *Rotor Dynamics*, A Halsted Press Book, pp. 219–225.

Vance, J. M., 1988, *Rotordynamics of Turbomachinery*, John Wiley and Sons, pp. 347–361.

APPENDIX

Dynamic Moments Acting on Rotor

The dynamic moment acting on the rotor about point C in Fig. 4(*b*) is obtained by

$$\Sigma \mathbf{M}_C = \mathbf{r}_{G/C} \times m\mathbf{a}_C + \frac{d}{dt}\mathbf{H}_C \tag{A1}$$

where $\mathbf{H}_C$ is the angular momentum of the rotor, $\mathbf{a}_C$ is the acceleration of point C, and $\mathbf{r}_{G/C}$ represents the imbalance, ϵ. A detailed discussion of the various coordinate systems is given by Green (1989, 1990). The coordinate systems that are used here completely conform with those defined in the previous papers. Only three coordinate systems are needed, however, to derive the dynamic moments that act on the rotor. These are:

$\xi\eta\zeta$—is an inertial coordinate system such that ζ and Z coincide, where both represent the axis of shaft rotation, Fig. 4(*b*).

XYZ—is attached to the shaft which rotates about Z at a speed, ω. The angle between X and ξ is ωt, Fig. 5.

xyz—is the rotor reference system where the rotor nutation, γ_r, takes place about x. Axis x is parallel to the XY plane. The xy plane is parallel to the rotor plane, Fig. 4(*b*). The angle between x and ζ is $\psi_r = \omega t + \psi$, Fig. 5.

$(d/dt)\mathbf{H}_c$ of Eq. (A1) is given in Eq. (6) in Green (1990) with the approximations of $\sin \gamma_r \approx \gamma_r$ and $\cos \gamma_r \approx 1$:

$$\frac{d}{dt}\mathbf{H}_C = \begin{Bmatrix} I_t\ddot{\gamma}_\xi + I_p\omega\dot{\gamma}_\eta \\ I_t\ddot{\gamma}_\eta - I_p\omega\dot{\gamma}_\xi \\ 0 \end{Bmatrix}_{\xi\eta\zeta} \tag{A2}$$

The transformation matrix, $[R]$, from the $\xi\eta\zeta$ system to the xyz system is defined as

$$[R] = \begin{bmatrix} \cos\psi_r & \sin\psi_r & 0 \\ -\sin\psi_r & \cos\psi_r & \gamma_r \\ \gamma_r \sin\psi_r & -\gamma_r\cos\psi_r & 1 \end{bmatrix} \tag{A3}$$

$\mathbf{r}_{G/C}$ is obtained as

$$\mathbf{r}_{G/C} = [R]^{-1}\begin{Bmatrix} \epsilon\cos\alpha \\ \epsilon\sin\alpha \\ 0 \end{Bmatrix}_{xyz} = \begin{Bmatrix} \epsilon\cos\alpha_r \\ \epsilon\sin\alpha_r \\ \epsilon\gamma_r\sin\alpha \end{Bmatrix}_{\xi\eta\zeta} \tag{A4}$$

where α and α_r are the relative and absolute precessions of ϵ with respect to x and ξ, respectively, Fig. 5. The position vector of C with respect to O is obtained as

$$\mathbf{r}_{C/O} = [R]^{-1}\begin{Bmatrix} 0 \\ 0 \\ d \end{Bmatrix}_{xyz} = \begin{Bmatrix} d\gamma_\eta \\ -d\gamma_\xi \\ d \end{Bmatrix}_{\xi\eta\zeta} \tag{A5}$$

where $\gamma_\xi = \gamma_r \cos\psi_r$, and $\gamma_\eta = \gamma_r \sin\psi_r$. Then, $\mathbf{a}_c$ is obtained as the second time derivative of Eq. (A5). Hence,

$$\mathbf{a}_C = \frac{d^2}{dt^2}\mathbf{r}_{C/O} = \begin{Bmatrix} d\ddot{\gamma}_\eta \\ -d\ddot{\gamma}_\xi \\ 0 \end{Bmatrix}_{\xi\eta\zeta} \tag{A6}$$

Using Eqs. (A4) and (A6), the first term in RHS of Eq. (A1) is obtained as

$$\mathbf{r}_{G/C} \times m\mathbf{a}_C = \begin{Bmatrix} md\epsilon\gamma_r\ddot{\gamma}_\xi\sin\alpha \\ md\epsilon\gamma_r\ddot{\gamma}_\eta\sin\alpha \\ -md\epsilon(\ddot{\gamma}_\xi\cos\alpha_r + \ddot{\gamma}_\eta\sin\alpha_r) \end{Bmatrix}_{\xi\eta\zeta} \tag{A7}$$

Finally, substituting Eqs. (A2) and (A7) into Eqs. (A1) the dynamic moments acting on the rotor about C are

$$\Sigma\mathbf{M}_C = \begin{Bmatrix} (I_t + md\epsilon\gamma_r\sin\alpha)\ddot{\gamma}_\xi + I_p\omega\dot{\gamma}_\eta \\ (I_t + md\epsilon\gamma_r\sin\alpha)\ddot{\gamma}_\eta - I_p\omega\dot{\gamma}_\xi \\ -md\epsilon(\ddot{\gamma}_\xi\cos\alpha_r + \ddot{\gamma}_\eta\sin\alpha_r) \end{Bmatrix}_{\xi\eta\zeta} \tag{A8}$$